

Injection luminescence from CdS(11 $\bar{2}$ 0) studied with scanning tunneling microscopy

R. Berndt and J. K. Gimzewski

IBM Research Division, Zurich Research Laboratory, 8803 Rüschlikon, Switzerland

(Received 23 September 1991)

We have used a scanning-tunneling-microscope tip as a source of both electrons and holes to study injection luminescence from CdS(11 $\bar{2}$ 0) surfaces cleaved in UHV. Band-gap radiation and emission from radiative deep levels are resolved in optical spectra. Isochromat photon-intensity spectra exhibit, as a function of negative tip voltage, discrete steps which are discussed in terms of pair-creation thresholds. For positive tip polarity, hole creation in the valence band results in a continuous increase in the luminescence. Spatial maps of the resulting integrated light intensity acquired simultaneously with the conventional topographs reveal subnanometer-scale image contrasts which are attributed to defects, such as dislocations or radiative deep levels.

I. INTRODUCTION

Scanning tunneling microscopy (STM) has been widely used to obtain high-resolution images of *surface* geometric and electronic properties of metals and semiconductors.¹ The tunneling current which usually serves as the only source of information is determined predominantly by the surface density of states. However, on semiconductor materials, a bulk contribution to the current can be present when a high electric field between the tip and sample induces band bending. Consequently, in addition to the vacuum tunnel gap, a depletion region can extend into the crystal (depending on the sample conductivity and bias conditions).² Subsurface properties of buried interfaces can be studied more directly with ballistic electron emission microscopy.³ In a previous report on light emission from the STM,⁴ we suggested that luminescence emission from semiconductors could be used to map local defects and band-gap emission. Subsequently, spatial mapping of light emission intensities has been applied to investigate metallic surfaces⁵⁻⁸ and to image Al_xGa_{1-x}As/GaAs heterostructures.⁹

The potential of II-VI semiconductor materials as light-emitting devices in the visible spectrum¹⁰ has generated much interest in their luminescence properties. In this paper, we examine luminescence from CdS(11 $\bar{2}$ 0) surfaces induced by the tip of a STM. We present experimental evidence that subsurface properties of wide-band-gap semiconductor materials can be directly investigated via photon emission. Optical spectra of the luminescence from CdS(11 $\bar{2}$ 0) are presented, from which identification of the emission processes that contribute to the total intensity are discussed. In relation to conventional *I-V* tunneling characteristics, the interpretation of the luminescence is found to be more direct. Isochromat spectra are used to elucidate the excitation mechanisms involved. Finally, spatial maps of luminescence intensity exhibiting contrast on a lateral scale, hitherto not achievable using conventional electron beam excitation, are discussed.

II. EXPERIMENTAL DETAILS

For the experiments described in this paper, we used a specially built photon STM described in detail elsewhere.⁶ Briefly, the experiments were performed in ultrahigh vacuum (UHV) ($p < 1 \times 10^{-10}$ Torr) at room temperature. Tips and samples were introduced via an air-lock without breaking the vacuum. Electrochemically etched tungsten tips were prepared by heating to ≈ 1100 K in vacuum followed by argon-ion bombardment and field desorption. Light emitted from the tip-surface region was collected using a condenser lens placed at an angle of 45° with respect to the surface normal close to the STM inside the vacuum chamber. The solid angle subtended was ~ 1 sr. Externally, the collimated light was detected using a multi-alkali-metal photomultiplier. Peltier cooling allowed a photon-counting mode to be achieved with a dark count rate lower than 30 counts/sec. Alternatively, a second lens was mounted to focus the light onto an optical fiber coupled to a grating spectrometer, and on an optical multichannel analyzer interfaced to a computer.

The lower and upper limits of photon energies are determined by detector response ($\lambda \approx 890$ nm) and window transmission ($\lambda \approx 340$ nm), respectively. Maps of integrated photon intensity (photon maps) were recorded simultaneously with topography using the photomultiplier configuration. Isochromat spectra were measured by introducing an optical filter (500 ± 35 nm full width at half maximum), which matches the band gap of CdS ($E_g = 2.58$ eV).¹¹

In this study, low resistivity ($\rho \approx 10$ Ω cm) single-crystal bars of hexagonal wurtzite-structure CdS were cleaved *in vacuo* so as to expose the (11 $\bar{2}$ 0) plane. This and the (10 $\bar{1}$ 0) face are the lowest-index, nonpolar crystal surfaces that serve as natural cleavage planes.¹² Cleavage results in a mixture of (10 $\bar{1}$ 0) and (11 $\bar{2}$ 0) facets containing a high density of steps. We studied various crystals and found that only a few samples cleaved adequately for STM work. Ohmic contacts were made using a eutectic

of Ga and Al.¹³ The position of the Fermi level E_F was determined from the work function $\phi=4.8$ eV (Ref. 12) and the phototreshold $\phi_\theta=7.2$ eV (Ref. 14) to be 2.4 eV above the valence-band maximum. Given an energy band gap of $E_g=2.58$ eV, the conduction-band minimum is situated 0.2 eV above E_F .

III. RESULTS

A. Optical spectra

Figure 1 shows optical spectra of the emitted light acquired at a tunneling current of $i_t=10$ nA. Light emission is observed with a negatively [tip voltage $V_t=-7$ V in 1(a), 1(b), and 1(d)] and a positively [$V_t=10$ V in 1(c)] biased tip. In all spectra a peak G at 490 nm (2.53 eV) and a broad band C centered around 700 nm (1.8 eV) are present. The relative strength of these features was observed to vary with lateral tip position. Peak G is attributed to luminescence generated via radiative recombination of electrons from levels close to the conduction-band edge with holes in the vicinity of the valence-band edge. At room temperature, the various contributions of radiation involving transitions between shallow impurities, exciton states, and the electronic bands result in spectral broadening. Typical energies for these radiative transitions range from 2.4 to 2.6 eV.¹¹ The broad emission band C observed at 1.8 eV is assigned to radiative deep impurity or defect levels such as Co^{2+} , Li, or S disturbed by a Cd vacancy.¹¹ The extrinsic emission of band C may be more intense than intrinsic luminescence [in Figs. 1(a) and 1(b)].¹⁵ Interestingly, the spectra obtained here show strong similarities with conventional cathodoluminescence (CL) studies¹⁶ at room temperature, although the energy of the incident electron is several orders of magnitude smaller in the STM experiment.

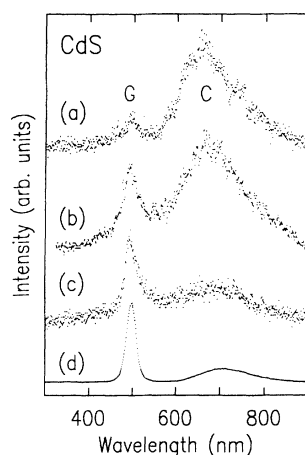


FIG. 1. Spectra of luminescence emitted from a STM observed at different tip positions on a CdS(11 $\bar{2}$ 0) surface. The spectra were acquired at $i_t=10$ nA and $V_t=-7$ V in (a), (b), and (d), and $V_t=+10$ V in (c) at varying lateral tip positions. Spectra were found to exhibit similar characteristics independent of tip bias. The relative intensity of luminescence due to band-edge emission (G) to emission from deep centers (C) varied with lateral tip position.

As the CdS samples are n -type semiconductors, the photon flux is limited by the rate of hole creation. In a CL experiment, holes are generated by impact ionization. This corresponds to negative values of V_t in our STM experiment [Figs. 1(a), 1(b), and 1(d)], as will be discussed in detail later. Additionally, in the STM, holes can be created directly through injection by applying V_t positive. Here, electrons tunneling to the tip leave holes in the CdS valence band; this is also found to result in luminescence [Fig. 1(c)].

B. I - V tunnel characteristics

Identifying spectral features in luminescence spectra is fairly straightforward. However, interpretation of I - V tunneling characteristics has proved to be a demanding task even for highly doped GaAs.¹⁷ Figure 2 displays I - V spectra measured on the same CdS sample by applying a voltage ramp to the tip while keeping the lateral tip position fixed. Simultaneously, the tip was linearly ramped toward the surface with a maximum excursion Δz of 4 Å as the bias voltage approached 0 V. This technique, developed by Mårtensson and Feenstra,¹⁸ was used to compensate approximately for the exponential decrease of current with V_t . In particular, detection of a small current contribution from defect states in the CdS band gap requires an increased transmission of the vacuum tunnel barrier by decreasing the tip-surface distance. Inspection of the experimental spectra in Fig. 2 reveals that no such gap states are observable in the I - V spectra, whereas they appear prominently in our optical spectra (Fig. 1). Furthermore, electrons from the CdS conduction band apparently do not contribute significantly to the tunneling current consistent with a low dopant density. Band-structure calculations¹⁹ have shown that the direct gap is confined to a small region in k space around $\bar{\Gamma}$, effectively prohibiting tunneling from the conduction-

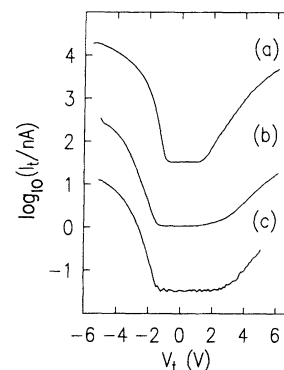


FIG. 2. I - V spectra measured at different lateral surface positions in one experimental run. Using a sample-and-hold function, the STM was regulated at $V_t=-4.9$ V and $i_t=1$ nA. The regulation was then disabled, the tip voltage was ramped, and the current recorded. Simultaneously, a linear ramp toward the surface was superimposed on the z piezoelectric with an initial offset of 1 Å increasing to 4 Å at zero bias and returning to 1 Å at the end of the scan. Spectra (a) and (b) have been offset by 3 and 1.5 decades, respectively. Instrumental noise corresponding to a current of 30 pA is present in all spectra.

band minimum.

In addition, the tunnel spectra exhibit a considerable variability in the apparent gap width. Whereas the expected CdS energy gap is resolved in Fig. 2(a), the gap appears substantially wider in Figs. 2(b) and 2(c). This variability in gap width was also reported on a smaller scale even for highly doped GaAs.¹⁷ In low-conductivity semiconductors, the potential between tip and sample drops over the gap and an extended region in the semiconductor giving rise to tip-induced band bending. Consequently, the tunneling barrier may extend well into the semiconductor, effectively obscuring the band onsets. Differences in tip work function between subsequent measurements can also modify the potential distribution.¹⁷ Therefore, on a wide-band-gap material with low dopant densities (and high dopant density fluctuations), the apparent gap position is ill-defined. As a result of the extended tunnel barrier inside the semiconductor, I - V spectra are not purely surface sensitive but may contain significant contributions from local subsurface properties.

C. Isochromat spectra

More insight into the excitation mechanism for luminescence can be obtained from isochromat spectra of the photon intensity as a function of the applied bias obtained using an optical filter to limit the detector response to energies close to E_g . Figure 3 shows isochromat spectra as a function of V_t recorded at constant current i_t . For positive V_t [Fig. 3(a)], a threshold for light emission at $h\nu=2.5$ eV is found at ≈ 2.5 eV and with increasing bias the photon-emission intensity increases continuously. For negative V_t [Fig. 3(b)], a first threshold is found close

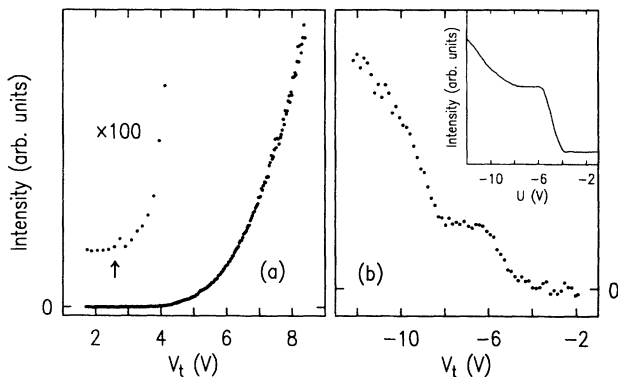


FIG. 3. Intensity of band-edge emission (isochromat spectra) as a function of applied tip bias, recorded at constant current $i_t = 1$ nA. (a) For positive tip bias a continuous increase of light intensity is observed. As evident from the inset showing the low-voltage region on a larger scale, light emission sets in smoothly above a threshold close to the energy gap $E_g = 2.58$ eV of CdS. As discussed in the text, a threshold of 2.4 eV (arrow) corresponding to the position of the valence-band maximum is expected. (b) For negatively biased tip, light emission is found above a threshold at $V_t = -4$ V. The intensity saturates in the region from $V_t = -6$ V up to a second threshold at $V_t = -8$ V where a second increase in intensity begins. The inset shows the result of the model calculation by Alig *et al.* (Ref. 22).

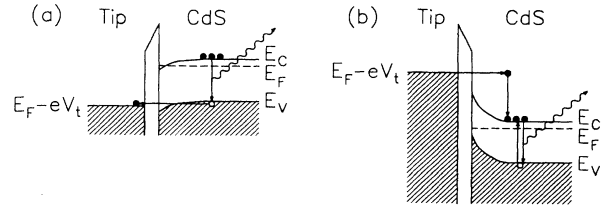


FIG. 4. Energy diagrams of the tunneling junction for positively (a) and negatively (b) biased tips. On low-conductivity materials, strong tip-induced band bending is expected, indicated schematically in the figure. It should be noted that the effect of momentum conservation discussed in the text has been omitted from (b) for simplicity.

to $V_t = -4$ V. Between $V_t = -6$ and -8 V, the luminescence intensity forms a plateau and then increases further beyond a second threshold at $V_t \approx -8$ V.

The isochromat spectra observed experimentally can be interpreted using an energy diagram of the tunneling junction shown in Fig. 4. In the case of $V_t > 0$ [Fig. 4(a)], holes are created by electrons tunneling from the CdS valence band to the tip. A negligible fraction of i_t is carried by electrons from the conduction band tunneling to the tip as can be judged from the I - V tunneling spectra. Since the CdS Fermi level lies in the proximity of the conduction-band edge, a threshold for emission is found for $eV_t \approx E_g$. For a negatively biased tip [Fig. 4(b)], the hot electron injected from the tip can create a hole in the valence band by impact ionization. Assuming that the impact ionization not only conserves the energy but also the momentum, we estimated the threshold energy for creation of a single electron-hole pair E_{e-h} within a simple model of free particle bands. Using the $\frac{1}{2}$ -band-gap rule,²⁰ we obtain $E_{e-h} = -3.9$ eV. The hot electron-hole pair relaxes to the band edges before recombination occurs,²¹ giving rise to band-edge luminescence. Above $V_t = 6.7$ V,²² the electron can create two holes, giving rise to the second threshold in the photon yield observed in Fig. 4(b).

The photon intensities observed can be estimated to result from external quantum efficiencies of $\sim 10^{-5}$ photons per electron at $V_t = +6$ V and $\sim 10^{-7}$ photons per electron at $V_t = -6$ V, assuming isotropic emission. Our isochromat spectra for negative V_t are in good qualitative agreement with data from Steinrisser,²³ who measured the luminescent intensity at $\lambda = 523$ nm from CdS surfaces as a function of energy using conventional electron beams. In addition, quantum yield calculations of isochromat spectra performed by Alig, Bloom, and Struck,²² shown in the inset of Fig. 3(b), follow our experimental data very closely.

D. Photon mapping

So far, we have concentrated on the spectral characteristics of luminescence detected from the STM, and discussed the mechanisms responsible for excitation and emission. We shall now focus on the use of the STM to map the emitted-light intensity as a function of lateral tip

position simultaneously with the topography of a surface analogous to a CL experiment, using a scanning electron microscope (SEM). A representative example of this mode of operation is presented in Fig. 5. Figure 5(a) shows the topography of a $200 \times 100 \text{ \AA}^2$ area of

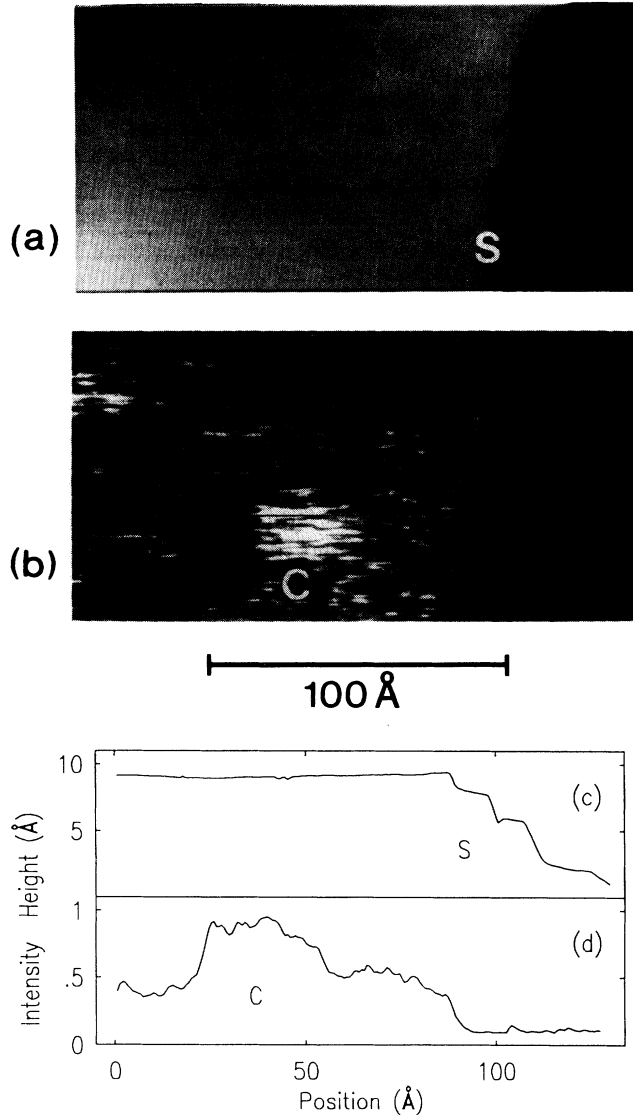


FIG. 5. (a) Conventional STM topograph represented as a gray-scale image taken from a $200 \times 100 \text{ \AA}^2$ region of CdS(11 $\bar{2}$ 0) at $V_t = -7 \text{ V}$ and $i_t = 5 \text{ nA}$. An atomically flat region (left) and a stepped area (right) can be recognized. (b) Integrated photon intensity recorded simultaneously with topography. Gray scale corresponds to 0 to 1000 counts/sec. Photon yield is fairly constant from the flat surface region. It drops to the experimental noise level, however, in the stepped surface area. A spot of enhanced luminescence (marked C) is apparent in the photon map. (c) and (d) Cross sections of topograph and photon map taken at the positions marked in (a). The topography is flat to within 0.1 \AA on the left. On the right a staircase S of a single, a double, and a triple atomic step is visible. The light intensity drops by a factor of 10 in the stepped region, whereas the emission is enhanced by a factor of 2 on the spot C with respect to the signal from the flat surface.

CdS(11 $\bar{2}$ 0) represented as a gray-scale image. The surface topography is observed to be atomically flat with the exception of a stepped region S on the right-hand side of the image. A cross section of the topography [marked with a line in Fig. 5(a)] is shown in Fig. 5(c). Region S consists of a staircase of mono-, double-, and triple-atomic steps. The region on the left is featureless down to a subangstrom level. Figure 5(b) displays a simultaneously recorded map of the integrated photon intensity. Here the gray scale represents intensity from 0 (black) to 1000 counts/sec (white). Fairly homogeneous emission is observed on the flat region in the lower half of the image. Additionally, a $\approx 40\text{-\AA}$ -diameter spot of higher intensity is visible in the center of the photon map. On the stepped area S, significantly less light is detected. Figure 5(c) shows a cross section through the topographic image [Fig. 5(b)], and the corresponding cross section of the photon map is shown in Fig. 5(d). We note that the intensity of detected emission increases by a factor of 2 over region C, occurring over a lateral distance of only $\sim 6 \text{ \AA}$. A drastic reduction can also be observed in the stepped region S.

Interpretation of the image contrast mechanism at the photon maps on the nanometer or subnanometer scale should be approached with care. The existing interpretations of CL images obtained using a SEM are usually concerned with features on the micrometer or submicrometer scale. Since the surfaces studied in this experiment were cleaved from bulk crystals, we tentatively reject the possibility that the observed steps are affected by an aggregation of point defects as could be the case for steps existing during crystal growth. Rather, we attribute the decreased luminescence yield to the steps themselves. Possible mechanisms are a modification of the probabilities for pair creation or the opening of nonradiative channels for energy dissipation. The sharpness of contrast in the light intensity suggests an injection-related mechanism. In the case of steps, the simultaneously recorded topographies permit correlation of photon emission with surface structure. In contrast, no surface topographic feature is found in Fig. 5(a), which correlates with the enhanced yield observed in region C of Fig. 5(b). Consequently, we can attribute the enhanced emission to the presence of a subsurface defect that changes the emission or hole creation rates such as a radiative deep level. As shown in Fig. 1, intense emission from these levels is observed in the optical spectra. Zero-dimensional defects or dislocations are known to influence image contrast in CL maps.¹⁵ An important open question in CL studies is whether contrast at dislocations is due to the dislocation core itself or is caused by a Cottrell atmosphere²⁴ of point defects.¹⁵ In our experiment the small lateral extent of the structure C indicates a very confined defect which suggests that Fig. 5(b) shows a dislocation core or the first observation of an individual radiative deep level.

IV. CONCLUSION

By operating a scanning tunneling microscope at positive or negative tip bias, we have shown that hole injection or impact ionization by electrons can lead to

luminescence from CdS(11 $\bar{2}$ 0) surfaces. In good agreement with electron-beam experiments, intrinsic and extrinsic luminescence are generated and are spectrally resolved. Luminescence spectra provide a sensitive and high-resolution probe for defect levels compared with conventional I - V spectroscopy, as has been demonstrated. Variations in photon intensity related to bulk and surface defects are observed on a subnanometer scale. We have shown that subsurface properties strongly influence the luminescence spectra and image contrast on this wide-band-gap semiconductor. Luminescence studies with a STM at low temperatures should allow higher spectral resolution of the unbroadened luminescence and thus

permit a more-detailed study of crystal defects and their impact on luminescence properties.

ACKNOWLEDGMENTS

We would like to thank D. Abraham, O. Albrektsen, A. Jakubowicz, P. Koenraad, H. W. M. Salemink, and J. Spence for useful discussions. In particular, we are grateful to K. O. Magnusson for many discussions and for help with sample preparation, and to I. Broser for providing some of the crystals used in our cleavage studies. The support of H. Rohrer, E. Courtens, and B. Reihl is gratefully acknowledged.

-
- ¹For recent reviews on scanning tunneling microscopy and spectroscopy of metal and semiconductor surfaces, see R. J. Behm, in *Scanning Tunneling Microscopy and Related Methods*, edited by R. J. Behm, N. Garcia, and H. Rohrer, NATO Advanced Study Institute Series E: Applied Sciences (Kluwer, Dordrecht, 1990), Vol. 184, pp. 173–210; R. M. Feenstra, *ibid.*, pp. 211–240.
- ²R. M. Feenstra and J. A. Stroscio, *J. Vac. Sci. Technol. B* **5**, 923 (1987).
- ³W. J. Kaiser and L. D. Bell, *Phys. Rev. Lett.* **60**, 1406 (1988).
- ⁴J. K. Gimzewski, B. Reihl, J. H. Coombs, and R. R. Schlittler, *Z. Phys. B* **72**, 497 (1988).
- ⁵R. Berndt, A. Baratoff, and J. K. Gimzewski, in *Scanning Tunneling Microscopy and Related Methods* (Ref. 1), pp. 269–280.
- ⁶R. Berndt, R. R. Schlittler, and J. K. Gimzewski, *J. Vac. Sci. Technol. B* **9**, 573 (1991).
- ⁷R. Berndt, R. R. Schlittler, and J. K. Gimzewski, in *Scanned Probe Microscopies-STM and Beyond, Proceedings of the Engineering Foundation Conference, Santa Barbara*, edited by H. K. Wickramasinghe, AIP Conf. Proc. No. 241 (AIP, New York, 1992).
- ⁸R. Berndt, J. K. Gimzewski, and P. Johansson, *Phys. Rev. Lett.* **67**, 3796 (1991).
- ⁹D. L. Abraham, A. Veider, Ch. Schönenberger, H. P. Meier, D. J. Arent, and S. F. Alvarado, *Appl. Phys. Lett.* **56**, 1564 (1990).
- ¹⁰Y. S. Park and B. K. Shin, in *Electroluminescence*, edited by J. I. Pankove (Springer, Berlin, 1977), p. 133.
- ¹¹*Numerical Data and Functional Relationships in Science and Technology, Physics of II-VI and I-VII Compounds, Semimag-*
- netic Semiconductors*, Landolt-Börnstein, New Series, Vol. 17b (Springer, Berlin, 1982).
- ¹²K. O. Magnusson, S. A. Flodström, P. Mårtensson, J. M. Nicholls, U. O. Karlsson, R. Engelhardt, and E. E. Koch, *Solid State Commun.* **55**, 643 (1985).
- ¹³K. O. Magnusson, Ph.D. thesis, University of Lund, Sweden, 1987.
- ¹⁴N. J. Shevchik, J. Tejada, M. Cardona, and D. W. Langer, *Phys. Status Solidi B* **59**, 87 (1973).
- ¹⁵B. G. Yacobi and D. B. Holt, *J. Appl. Phys.* **59**, R1 (1986).
- ¹⁶D. B. Holt, *Microscopy of Semiconducting Materials*, IOP Conf. Proc. No. 76 (IOP, Oxford, 1981), p. 316.
- ¹⁷H. W. M. Salemink, O. Albrektsen, and P. Koenraad, *Phys. Rev. B* **45**, 6946 (1992).
- ¹⁸P. Mårtensson and R. M. Feenstra, *Phys. Rev. B* **39**, 7744 (1989).
- ¹⁹T. K. Bergstresser and M. L. Cohen, *Phys. Rev.* **164**, 1069 (1967).
- ²⁰P. A. Wolff, *Phys. Rev.* **95**, 1415 (1954).
- ²¹N. W. Ashcroft and N. D. Mermin, *Solid State Physics* (Holt-Saunders, Philadelphia, 1976).
- ²²R. C. Alig, S. Bloom, and C. W. Struck, *Phys. Rev. B* **22**, 5565 (1980).
- ²³F. Steinrisser, *Phys. Rev. Lett.* **24**, 213 (1970).
- ²⁴“The elastic interaction of point defect with the dislocation leads to the formation of ‘clouds’ of point defects called a Cottrell atmosphere.” See A. M. Kosevich, in *Dislocations in Solids*, edited by F. R. N. Nabarro (North-Holland, Amsterdam, 1979), Vol. I, p. 37.

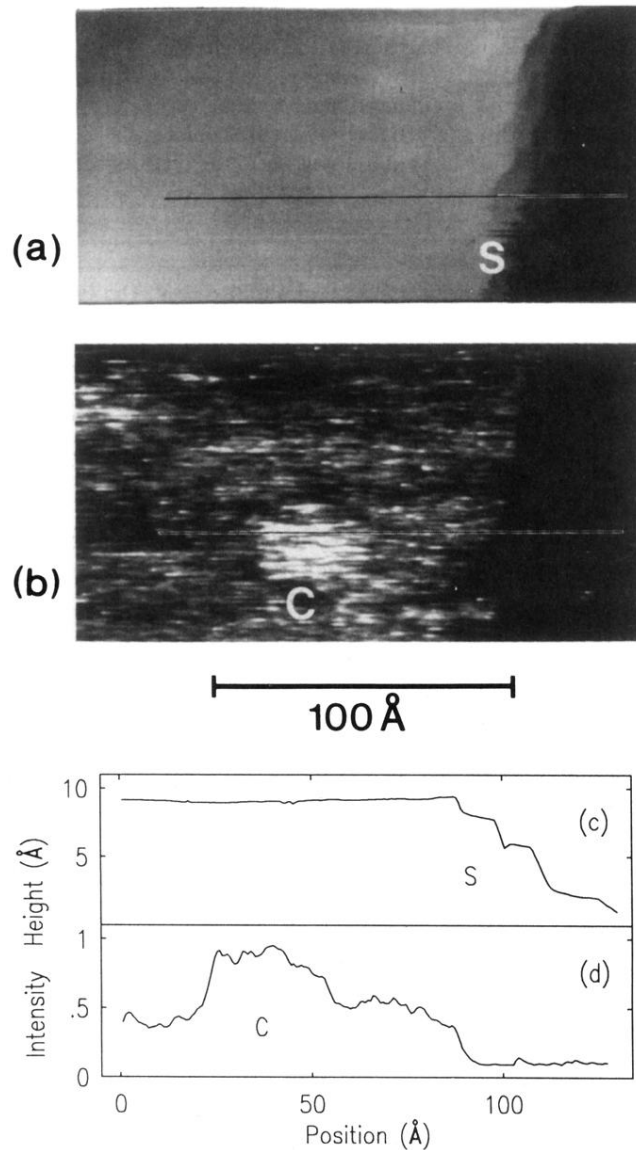


FIG. 5. (a) Conventional STM topograph represented as a gray-scale image taken from a $200 \times 100 \text{ \AA}^2$ region of $\text{CdS}(11\bar{2}0)$ at $V_t = -7 \text{ V}$ and $i_t = 5 \text{ nA}$. An atomically flat region (left) and a stepped area (right) can be recognized. (b) Integrated photon intensity recorded simultaneously with topography. Gray scale corresponds to 0 to 1000 counts/sec. Photon yield is fairly constant from the flat surface region. It drops to the experimental noise level, however, in the stepped surface area. A spot of enhanced luminescence (marked C) is apparent in the photon map. (c) and (d) Cross sections of topograph and photon map taken at the positions marked in (a). The topography is flat to within 0.1 \AA on the left. On the right a staircase S of a single, a double, and a triple atomic step is visible. The light intensity drops by a factor of 10 in the stepped region, whereas the emission is enhanced by a factor of 2 on the spot C with respect to the signal from the flat surface.